

# FGN: Fusion Glyph Network for Chinese Named Entity Recognition

Zhenyu Xuan, Rui Bao, Chuyu Ma, Shengyi Jiang<sup>\*</sup>

School of Information Science and Technology, Guangdong University of Foreign Studies, China

xuanzhenyu@foxmail.com, jiangshengyi@163.com

## Abstract

Chinese NER is a challenging task. As pictographs, Chinese characters contain latent glyph information, which is often overlooked. In this paper, we propose the FGN<sup>1</sup>, Fusion Glyph Network for Chinese NER. This method may offer glyph information for fusion representation learning with BERT. The major innovations of FGN include: (1) a novel CNN structure called CGS-CNN is proposed to capture glyph information from both character graphs and their neighboring graphs. (2) we provide a method with sliding window and Slice-Attention to extract interactive information between BERT representation and glyph representation. Experiments are conducted on four NER datasets, showing that FGN with LSTM-CRF as tagger achieves new state-of-the-arts performance for Chinese NER. Further, more experiments are conducted to investigate the influences of various components and settings in FGN.

## Introduction

Named entity recognition (NER) is generally treated as sequence tagging problem and solved by statistical methods or neural networks. Character-based tagging method is the main strategy on Chinese NER [Lu et al., 2016, Meng et al., 2019]. Furthermore, researches [Liu et al., 2010; Li et al., 2014] have explicitly compared character-based methods and word-based methods, confirming that the former are the better one. Therefore, representation learning toward character-level is essential for Chinese NER and this field has been explored widely.

Currently, distributed representation learning has been the mainstream method to represent Chinese characters, especially after the raise of BERT [Devlin et al., 2019], which raised the baselines for almost all fields of NLP. However, these methods overlooked the information inside words or characters. Actually, there have been studies, focusing on internal components of words or characters. In English field, researchers [Ma and Hovy, 2016] used Convolutional Neural Network (CNN) to encode the spelling of words as representation for NER task. This method is not suitable for Chinese NER, as Chinese is not alphabetical language but hiero-

glyphic language. Fortunately, Chinese characters can be further segmented into radicals. For example, character of “抓”(grasp) is consisted of “扌”(hand) and “爪”(claw). Study on radical-based character embedding [Sun et al., 2014] has confirmed the effectiveness of these components in Chinese characters.

Further, some researchers turn attention to regard Chinese characters as graphs for encoding. Researches [Dai and Cai, 2017] tried running CNNs on character graphs to obtain glyph representations and test the effectiveness in various downstream modeling tasks. However, the incorporation of glyph representations worsened the performance in their experiment. A similar CNN structure [Shao et al., 2017] was run to extract glyph representations and combined them with radical representations for CWS and POS tagging tasks. But their method performed ignorable improvement on multiple data sets. Avoiding the shortcomings of previous works, a glyph representation call Glyce [Meng et al., 2019] was proposed. Being Combined with BERT representation, Glyce achieved SOAT performances in various NLP tasks including NER. This method provided an ensemble of seven historical and contemporary scripts to enrich glyph information for each character and applied a Tianzige-CNN (田字格) structure to encode character graphs. Tianzige is a traditional form of Chinese calligraphy which conforms radical distribution of Chinese characters. Then Transformer [Vaswani et al., 2017] was used in Glyce to further encode character representations of BERT and Tianzige-CNN on Chinese NER.

We consider that Glyce is still deficient on NER task by below problems: (1) patterns of modern Chinese named entities are different from the ones in ancient time, as bronzeware script used in Glyce contains only 2420 characters that are verified but modern Chinese contains more than 7000 common characters. (2) Tianzige-CNN separately encodes each character graph, ignoring glyph information from neighboring characters. For example, characters in tree names like “杨树”(aspen), “柏树”(cypress) and “松树”(pine tree) have the same radical “木”(wood), but characters of an algorithm name “决策树”(decision tree) have no such pattern. (3) They only concatenated BERT representation and Glyce representation as input of subsequent network layer, but interactive information between two representations was overlooked. Actually, representation fusion methods [Zadeh et al., 2017; Zadeh et al., 2018; Mai et al., 2019] have got wide attention

<sup>\*</sup> corresponding author (jiangshengyi@163.com)

<sup>1</sup> <https://github.com/AidenHuen/FGN-NER>

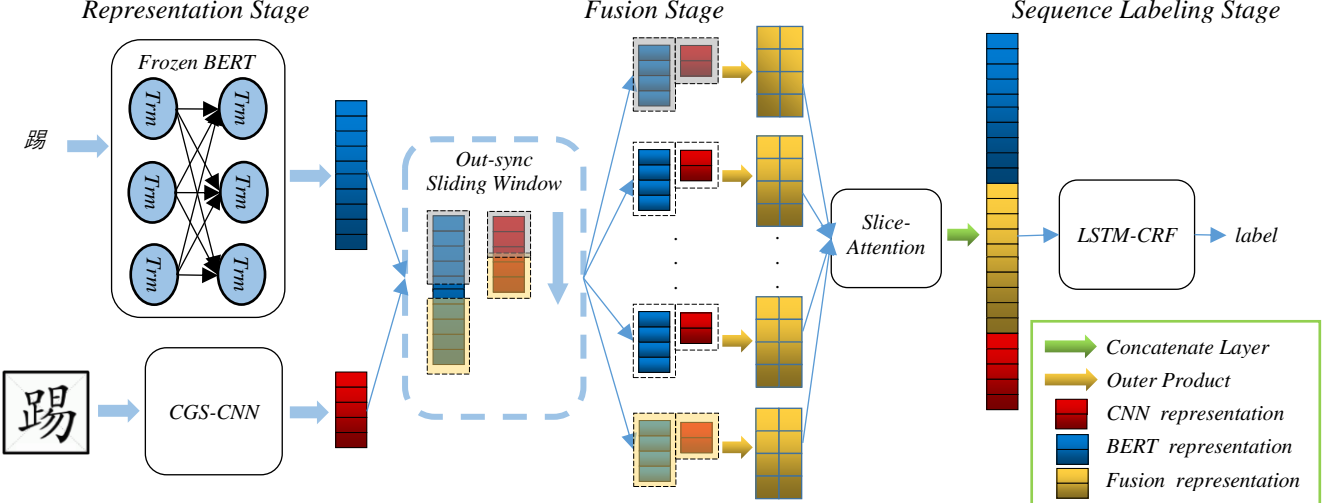


Figure 1: Architecture of the FGN for named entity recognition

in language modeling field, which are worth taking as reference for character-level vector fusion.

Therefore, we propose the FGN, Fusion Glyph Network for Chinese NER. Key techniques in FGN include: (1) a novel CNN structure called CGS-CNN, Character Graph Sequence CNN is proposed for glyph encoding. Only requiring one Chinese script, CGS-CNN may encode glyph information from both character graphs and their neighboring graphs. (2) We provide a fusion method with out-of-sync sliding window and Slice-Attention to extract interactive information between glyph representation and character representation. (3) BiLSTM-CRF is selected as sequence tagger for NER.

FGN is found to improve the performance of NER, which outperforms other SOAT models on four NER datasets (Section 4.2). We also encode radicals of characters to further enhance the performance of FGN, which tries confirming the complementation between glyph and radical representation. In addition, we verify and discuss the influence of various proposed settings in FGN (Section 4.3).

## 2 Related Work

Our work is related to neural network for NER. CNN-CRF model [Collobert et al., 2011] is a neural NER model, obtaining competitive result to various best statistical models. LSTM-CRF [Huang Z et al., 2015] has been widely used in current sequence labeling tasks, being the mainstream component in subsequent NER models. To obtain more word-level information, LSTM-CNN-CRF [Ma and Hovy, 2016] is proposed, using CNNs to encode the spelling of each English word. Further, a coreference aware representation learning method [Dai et al., 2019] was used and combined with LSTM-CNN-CRF for NER. In Chinese field, researches [Dong et al., 2016] organized radicals in each character as sequence and used LSTM to encode them on Chinese NER task. A novel NER method call lattice-LSTM [Zhang and Yang, 2018] was proposed, which skillfully encoded Chinese characters as well as all potential words that match a lexicon. Similar to Lattice-LSTM, Word-Character LSTM (WC-

LSTM) [Liu et al., 2019] was proposed, outperforming other SOAT NER models without BERT. WC-LSTM added word information into the start and the end characters of a word, alleviating the influence of word segmentation errors.

Currently, knowledge from vision has been widely-used leveraged in NLP. We simply divide these relative researches into two categories according to the source of vision knowledge: glyph representation learning and multimodal language modeling. The Former is scarce and Glyce [Meng et al., 2019] is one of these studies to obtain a significant boost. To our knowledge, we are the first to run 3D convolution to encode character graphs in sentence-level. Actually, 3D convolution is mostly provided to encode video information. Similar to video preprocessing, we transform text sentences to graph sequences. The latter is current hotspot in various NLP fields. Researchers [Zhang et al., 2018] proposed an adaptive co-attention network for tweets NER, which adaptively balanced the fusion proportions of image representation and text representation from a tweet. With reference of BERT, a multimodal BERT [Jiang et al., 2019] was proposed for target-oriented sentiment classification. Multiple self-attention layers [Vaswani et al., 2017] were used in the model to capture interactive information after concatenating BERT and visual representation. Further, Researchers [Mai et al., 2019] proposed a fusion network with local and global perspective for multimodal affective computing. They provided a sliding window to slice multimodal vectors and fused each slice pair by outer product. Also, Attentive Bi-directional Skip-connected LSTM was used to combine slice pairs. Our method borrows the ideas of above-mentioned methods for multimodal fusion. Different from theirs that fused the sentence-level representation, we focus on character-level fusion for Chinese NER.

## 3 Model

In this section, we introduce the FGN for NER task in detail. As shown in Figure 1, FGN can be divided into three stages:

representation stage, fusion stage and tagging stage. We follow the strategy of character-based sequence tagging for Chinese NER.

### 3.1 Representation Stage

We mainly use character representation and glyph representation, which are separately encoded by BERT and CGS-CNN. In addition, we encode radicals of each character for further experiment between glyph representation and radical representation. Detail of these representations are as followed.

#### Frozen BERT

BERT is a multi-layer Transformer encoder in nature, which offers distributed representations for words or characters. We use the pre-trained character-based BERT to encode each character in sentence. Different from the normal fine-tuning strategy, we first fine-tune BERT in training set with a CRF layer as tagger. Then freeze the BERT parameters and transfer them to another BERT structure, which is a part of the FGN. The reason to follow this strategy is that fine-tuning BERT only requires minimal learning rate but initialized parameters of FGN need a hundred times larger learning rate to adjust. Subsequent experiment shows the effectiveness of this strategy.

#### CGS-CNN

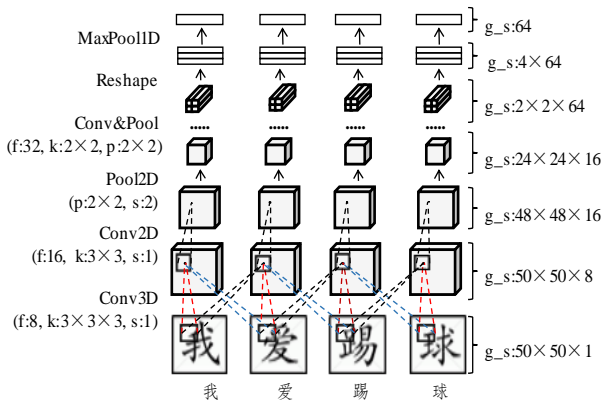


Figure 2: Architecture of CRS-CNN with a input sample “我爱踢球”(I love playing football). “f”, “k”, “s”, “p” stand for kernel number, kernel size, stride, and pooling window size. “g\_s” represents the tensor size of output from each layer.

Figure 2 depicts the architecture of CGS-CNN. Different from Glyce using seven types of character script, we only choose the simple Chinese script to generate glyph vectors. The input format of CGS-CNN is sentence but not single character. We first convert sentences to graph sequences, in which characters are replaced with  $50 \times 50$  gray-scale graphs. Characters that are not Chinese are given corresponding random matrices with values between 0 and 1. Then, we provide two  $3 \times 3 \times 3$  3D convolution layers to encode graph sequence and output each  $50 \times 50$  graph with 8 channels. 3D convolution can extract feature from both spatial and temporal dimensions, which means each glyph vector may obtain additional glyph information from the neighboring graphs. Using padding on the dimension of graph sequence, we may keep the

length of graph sequence constant after passing through 3D convolution, which is necessary for character-based tagging. Then the output of 3D convolution passes through several groups of 2D convolution and 2D max pooling to compress each graph to  $2 \times 2$  Tianzige-structure with 64 channel. In order to filter noises and blank pixels, we then flatten the  $2 \times 2$  structures and adopt a 1D max pooling to extract glyph vector for each character. The size of glyph vectors is 64 that is much smaller than the size of Tianzige-CNN output (1024 dimension).

Different from Glyce that sets image classification task to learn glyph representation, we learn the parameters of CGS-CNN while training whole NER model in domain datasets. As we only use the simple Chinese script, setting task to predict the character IDs of this script seems meaningless.

#### Radical Representation

We organized Chinese character as radical sequence. For example, character “朝”(morning) can be divided into {“丶”(ten), “曰”(sun), “十”(plus), “月”(moon)}. Radical embedding for a character can be defined as  $r = \{r_1, r_2, \dots, r_{l-1}, r_l\}$ . Where  $l$  represents the number of radicals in character and  $r_1$  represents the embedding of the 1th radical. Then self-attention [Vaswani et al., 2017] is adopted to encode this radical embedding:

$$r' = \text{softmax}\left(\frac{rW^Q W^K^T r^T}{\sqrt{d^r}}\right) rW^V \quad (1)$$

Where  $W^Q, W^K, W^V$  represent the initialized weights for the input vectors. After that, pass through a max pooling layer to extract radical features and obtain the radical vector  $r_v$  for a character:

$$r_v = \text{pool}(r') \quad (2)$$

### 3.2 Fusion Stage

We provide a sliding window to slide through both character and glyph vectors. After the sliding window, we obtain slice pairs and compute outer product among these pairs to obtain local interactive features. Then Slice-Attention is adopted to balance the importance of each slice pair and combine them to output fusion vector.

#### Out-of-sync Sliding Window

Sliding window has been applied in multimodal affective computing [Mai et al., 2019] as mentioned above. The reason for using sliding windows is that directly fusing vectors with outer product would exponentially expand vector size, which increases space and time complexity for subsequent network. However, this method requires the multimodal representations to have the same size, which is not suitable to slide through both BERT vector and glyph vector. Because character representations of BERT have richer semantic information than glyph representations, requiring a bigger vector size. Here we provide an out-of-sync sliding window that can satisfy different vector sizes while keeping the same number of slices.

Assume that we have one Chinese character with character vector defined as  $c_v \in \mathbb{R}^{d^c}$  and glyph vector defined as  $g_v \in \mathbb{R}^{d^g}$ . Here  $d^c$  and  $d^g$  stand for the sizes of two vectors.

To keep the same number of the slices of these two vectors after passing through the sliding window, the setting of sliding window needs to meet the following limitation:

$$n = \frac{d^c - k^c}{s^c} + 1 = \frac{d^g - k^g}{s^g} + 1, n \in \mathbb{N}^* \quad (3)$$

Where  $n$  is a positive integer, standing for slice number of two vectors;  $k^c$  and  $s^c$  respectively stand for window size and stride of character vector.  $k^g$  and  $s^g$  respectively represent window size and stride for glyph vector. The strategy we use to satisfy this condition is to limit the hyper-parameters of sliding window such that  $d^c$ ,  $k^c$  and  $s^c$  are respectively an integral multiple of  $d^g$ ,  $k^g$  and  $s^g$ .

To get slice pairs, we first calculate the left border index of sliding window at each stride:

$$i \in \{1, 2, 3, \dots, n\} \quad (4)$$

$$p_{(i)}^c = s^c(i - 1) \quad (5)$$

$$p_{(i)}^g = s^g(i - 1) \quad (6)$$

Where  $p_{(i)}^c$  and  $p_{(i)}^g$  represent the boundary index of sliding window respectively for character and glyph vector at the  $i$ th stride. Then we can obtain each slice during the following formula:

$$c_{-S(i)} = \{c_{-v(p_{(i)}^c+1)}, c_{-v(p_{(i)}^c+2)}, \dots, c_{-v(p_{(i)}^g+k^c)}\} \quad (7)$$

$$g_{-S(i)} = \{g_{-v(p_{(i)}^g+1)}, g_{-v(p_{(i)}^g+2)}, \dots, g_{-v(p_{(i)}^g+k^g)}\} \quad (8)$$

Where  $c_{-S(i)}$  and  $g_{-S(i)}$  represent the  $i$ th slices respectively from two vectors;  $c_{-v(p_{(i)}^c+1)}$  stands for the value at  $(p_{(i)}^c + 1)$ th dimension of  $c_v$ .

In order to fuse the two slice in a local perspective, outer product is adopted to generate an interactive tensor, as shown in the formula:

$$m_i = \text{Outer}(c_{-S(i)}, g_{-S(i)}) \\ = \begin{bmatrix} c_{-v_{p_{(i)}^c+1}} g_{-v_{p_{(i)}^g+1}}, \dots, c_{-v_{p_{(i)}^c+k^c}} g_{-v_{p_{(i)}^g+k^g}} \\ \vdots \quad \ddots \quad \vdots \\ c_{-v_{p_{(i)}^g+k^g}} g_{-v_{p_{(i)}^g+1}}, \dots, c_{-v_{p_{(i)}^g+k^g}} g_{-v_{p_{(i)}^g+k^g}} \end{bmatrix} \quad (9)$$

Where  $m_i \in \mathbb{R}^{d^c \times d^g}$  stands for fusion tensor of the  $i$ th slice pair;  $c_{-v_{p_{(i)}^c+1}} g_{-v_{p_{(i)}^g+1}}$  represent product result between the  $p_{(i)}^c + 1$ th value in  $c_v$  and the  $p_{(i)}^g + 1$ th value in  $g_v$ . During outer product, we may obtain all product result among elements from two vectors.

Then we flatten tensor  $m_i$  to vector  $m'_i \in \mathbb{R}^{n \times (k^c k^g)}$ . Representation of slices for one character can be represented as:

$$m' = \{m'_1, m'_2, \dots, m'_{n-1}, m'_n\}, m' \in \mathbb{R}^{n \times (k^c k^g)} \quad (10)$$

Where  $m'$  contains  $n$  fusion vectors of slice pairs. The size of each vector is  $k^c k^g$ .

### Slice-Attention

Outer product enriches the interactive information for characters at the same time generates more noises, as many features are irrelevant. With reference to attention mechanism, we propose the Slice-Attention, which can adaptively quantify the importance of each slice pair and combined them to

represent a character. Importance of slice pair can be quantified as:

$$a_i = \frac{\text{exp}(\sigma(v) \odot \sigma(W^{slice} \odot m'_i + b^{slice}))}{\sum_{i=1}^n \text{exp}(\sigma(v) \odot \sigma(W^{slice} \odot m'_i + b^{slice})) + \epsilon} \quad (11)$$

Where  $a_i$  stands for importance value of the  $i$ th slice pair;  $\sigma$  is Sigmoid function and  $\odot$  is dot product. Sigmoid function here may limit the value range in vectors between 0 and 1, which ensures subsequent dot product computing meaningful.  $W^{slice} \in \mathbb{R}^{(k^c k^g) \times (k^c k^g)}$  and  $b^{slice} \in \mathbb{R}^{k^c k^g}$  stand for initialized weight and bias.  $v \in \mathbb{R}^{(k^c k^g)}$  is similar to the query in self-attention [Vaswani et al., 2017], which is another initialized weight we provide.  $\epsilon$  represents a fuzz factor with the value of 1e-7.

Finally, we fuse the vectors of slice pairs by weighted average computation and obtain fusion vector  $f_v$  for a character:

$$f_v = \sum_{i=1}^n a_i m'_i \quad (12)$$

### 3.3 Tagging Stage

We concatenate each vector in character-level before tagging. As the need of experiment, two groups of representation are set to represent each character. One is without radical representation defined as  $\text{concat}(f_v, g_v, c_v)$ , another is with radical vector defined as  $\text{concat}(f_v, g_v, c_v, r_v)$ . Representation of a sentence can be defined as  $x = \{x_1, x_2, \dots, x_\tau\}$ , where  $\tau$  stands for the length of sentence.

#### BiLSTM

LSTM (Long Short Terms Memory) units contain three specially designed gates to control information transmission along a sequence. To encode sequence information of  $x$ , we use a forward LSTM network to obtain forward hidden state and a backward LSTM network to obtain backward hidden state. Then the two hidden states are combined as:

$$h = \overrightarrow{\text{LSTM}}(x) \oplus \overleftarrow{\text{LSTM}}(x) \quad (13)$$

Where  $h = \{h_1, h_2, \dots, h_\tau\}$  is the hidden representation of characters and  $\oplus$  represents sum operation of corresponding values between two hidden states.

#### CRF

A standard CRF layer is used to decode the hidden representation above. Here CRF may enhance the binding among the neighboring tagging results. Assume that we have a sentence represented as  $s$ . The probability of tagging result  $y = \{l_1, l_2, \dots, l_\tau\}$  for  $s$  is computed as:

$$P(y|s) = \frac{\exp(\sum_{i=1}^\tau (W_{l_i}^{crf} h_i + b_{(l_{i-1}, l_i)}^{crf}))}{\sum_{y'} \exp(\sum_{i=1}^\tau (W_{l'_i}^{crf} h_i + b_{(l'_{i-1}, l'_i)}^{crf}))} \quad (14)$$

Where  $y'$  represents a possible label sequence;  $W_{l_i}^{crf}$  is the weight for  $l_i$ ; and  $b_{(l_{i-1}, l_i)}^{crf}$  is the bias from  $l_{i-1}$  to  $l_i$ .

After CRF decoding, we use first-order Viterbi algorithm to find the most probable label sequence for a sentence. Assume that there is a labeled set  $\{(s_i, y_i)\}_{i=1}^N$ , we can maximize the below log-likelihood function to train the whole model:

Model	Weibo			MSRA			Resume			OntoNote 4		
	P	R	F	P	R	F	P	R	F	P	R	F
Lattice-LSTM	53.04	62.25	58.79	93.57	92.79	93.18	93.57	92.79	93.18	76.35	71.56	73.88
WC-LSTM	52.55	67.41	59.84	94.58	92.91	93.74	95.27	95.15	95.21	76.09	72.85	74.43
Glyce	67.68	67.71	67.70	95.57	95.51	95.54	96.62	96.48	96.54	80.87	80.40	80.62
BERT baseline	66.88	67.33	67.12	94.97	94.62	94.80	96.12	95.45	95.78	78.01	80.35	79.16
FGN	68.00	<b>72.61</b>	<b>70.23</b>	95.45	<b>95.81</b>	95.64	96.49	97.08	96.79	<b>82.61</b>	81.48	82.04
			+2.90			+0.84			+1.01			+2.88
FGN-Radical	<b>69.21</b>	70.60	69.90	<b>95.79</b>	95.48	<b>95.73</b>	<b>96.67</b>	<b>97.09</b>	<b>96.88</b>	81.43	<b>83.46</b>	<b>82.39</b>
			+2.57			+0.93			+1.10			+3.23

Table 1: Detailed statistics of FGN compared with various SOAT models

$$L = \sum_{i=1}^N \log(P(y_i|s_i)) \quad (15)$$

## 4 Experiments

In this section, we first introduce the datasets we use and some setting of experiments. Then we set a comparison of the proposed model and various SOAT models to discuss the effectiveness of FGN. Further, we explore and discuss the influences of different factors in FGN. The metrics we use contain: Precision (P), Recall (R), F1-score (F) for NER.

### 4.1 Experimental Settings

#### Dataset

Four widely-used NER datasets are chosen for experiments, including OntoNotes 4, MSRA, Weibo and Resume. All of these Dataset is annotated with a BMES tagging scheme. Among them, OntoNotes 4 and MSRA are in news domain; Weibo is annotated from Sina Weibo, a social media in China. These three datasets only contain traditional name entities, such as location, personal name and organization. Resume was annotated from personal resumes with 8 types of named entities. All datasets have been preprocessed, which can be obtained from Google Drive<sup>2</sup>.

#### Character Embedding

Character-based BERT we use has been pre-trained by Google<sup>3</sup>. Following the default configuration, output vector size of each character is set to 764. Character graphs we used are collected from *Xinhua Dictionaries*<sup>4</sup> with the number of 8630. We covert these graphs to  $50 \times 50$  gray-scale graph. Radicals for each character are collected according to the work [Dong et al., 2016]. Max length of radicals for each character is set to 7 and the size of radical embedding is set to 32.

#### Hyper-Parameter Setting

We use dropout for both character graphs and radical embedding. Dropout rate for graph is set to 0.2 and the radical one is set to 0.3. The hidden size of LSTM is set to 764 and the dropout rate of LSTM is set to 0.5. As mentioned in Section 3.2, window size and stride in sliding window of character vector are respectively an integer multiple of the ones for glyph vectors. Thus, we set size and stride of the former to 96 and 8, and the later to 12 and 1 according to empirical study.

Adam is adopted as optimizer for both BERT fine-tuning and NER model training. Learning rates for fine-tuning condition and training condition are different. The former one is set to 0.000002, and the latter one is set to 0.002.

### 4.2 Main Result

Table 1 shows some detailed statistics of FGN, compared with other SOAT model on four NER datasets. Here FGN represents the proposed model without extra radical representation; FGN-Radical represents the proposed model with extra radical representation as mentioned in Section 3.1. Both FGN and FGN-radical apply BiLSTM-CRF as tagger. Lattice LSTM [Zhang and Yang, 2018] and WC-LSTM [Liu et al., 2019] are the SOAT model without BERT, combining both word embedding and character embedding. Glyce [Meng et al., 2019] is the SOAT BERT-based model as mentioned earlier. In addition, we set BERT as baseline in this experiment, as FGN is also based on pre-trained BERT.

As can be seen, FGN and FGN-Radical outperform other SOAT models in all four datasets. Compared with baseline model, the F1 of FGN obtains obvious boosts of 2.90%, 0.84%, 1.01% and 2.88% respectively on four datasets. Improvement of FGN is obvious on datasets with high recognition difficulty like Weibo and OntoNote 4. It confirms that FGN effectively fuse glyph information on the basis of BERT, which enhance the capability of character-level semantic representation on NER task. Especially, even only using simple Chinese script, FGN outperforms Glyce with boosts of 2.53%, 0.10%, 0.15% and 1.42% respectively on four datasets. Further, FGN-Radical slightly outperforms FGN in three datasets, except for Weibo, which is less formal in expression. It seems that glyph representation and radical representation are complementary in some cases. Actually, CGS-CNN mainly encodes the information of image pixels, which inevitably leaves out some information from radical.

### 4.3 Ablation Study

Here we discuss the influences of various settings and components in FGN. The components we investigate contain: CNN structure, named entity tagger and fusion method. Weibo dataset is used for these illustrations. In addition, we

<sup>2</sup> <https://drive.google.com/file/d/1mDKkc2-8e4wXAuAnGiZ-MHI59UgVb1q4/view>

<sup>3</sup> <https://github.com/google-research/bert>

<sup>4</sup> <http://zidian.aies.cn/>

investigate the performance of vision-based NER method without any distributed representation.

### Effect of CNN structure

As shown in Table 2, we investigate the performances of various CNN structures while keep other settings of FGN constant. In this table,  $2d$  represents the CGS-CNN with no 3D convolution layer.  $avg$  represents that 1D max pooling in CGS-CNN is replaced by 1D average pooling. 2D CNN represents the CNN structure with only 2D convolution and 2D pooling layers. Tianzige-CNN is proposed from Glyce.

CNN-type	P	R	F
CGS-CNN <sup>2d</sup>	67.56	70.45	69.01
CGS-CNN <sup>avg</sup>	68.13	70.35	69.22
2D-CNN	66.75	71.45	68.93
Tianzige-CNN	<b>69.94</b>	69.24	69.59
CGS-CNN	68.00	<b>72.61</b>	<b>70.23</b>

Table 2: Performances of various CNN structures on Weibo dataset

As can be seen, the common 2D-CNN structure obtains the worse result, as it completely overlooks the information of Tianzige structure and neighbor character glyph. Comparing with Tianzige-CNN, using CGS-CNN introduces a boost of 0.64% in F1. Using 3D convolution in CGS-CNN introduces a boost of 1.11% in F1. Further, max pooling works better than average pooling when capture feature in Tianzige structure. As mentioned earlier, max pooling may better filter some blank pixels and noises in character graph.

### Effect of Named Entity Tagger

Some widely-used sequence taggers are chosen to replace BiLSTM-CRF in FGN for discussion. Table 3 shows the performances of various chosen taggers. As can be seen, methods that based on LSTM and CRF outperform Transformer [Vaswani et al., 2017] encoder in NER task. Compared with only CRF, LSTM introduces a boost of 0.43% in F1. In addition, bidirectional LSTM introduces a further boost of 0.54% in F1.

tagger-type	P	R	F
CRF	69.44	69.10	69.26
LSTM-CRF	69.77	69.60	69.69
BiLSTM-CRF	68.00	<b>72.61</b>	<b>70.23</b>
Transformer	<b>72.14</b>	66.08	68.98

Table 3: Performances of various taggers on Weibo dataset

### Effect of Fusion Method

We investigate the performances of different setting in fusion stage as shown in Table 4. In this table, concat represents concatenating glyph and BERT representation without any fusion; no freeze represents FGN with trainable BERT; avg pool and max pool represent that Slice-Attention in FGN is respectively replaced by pooling or max pooling; outer-fc represents the FGN without sliding windows, applying outer product and a fully connected layer with 128 units to directly fuse the output of BERT and CGS-CNN. In addition, we reset the window size to (196, 16), (48, 4) and the stride to (24, 2)

in sliding window respectively for character and glyph representations.

fusion-type	P	R	F
concat	68.13	70.35	69.43
no freeze	65.92	<b>73.87</b>	69.67
avg pool	68.00	72.61	69.11
max pool	68.60	70.40	69.64
outer-fc	67.90	72.36	69.81
w(196, 16)	<b>69.58</b>	70.10	69.84
w(48, 4)	69.25	70.22	69.73
s(24, 2)	68.17	72.10	70.08
FGN	68.00	72.61	<b>70.23</b>

Table 4: Performances of different fusion settings on Weibo dataset

Compared to directly concatenating vectors from glyph and BERT, FGN introduces a boost of 0.80% in F1, confirming the effectiveness of our fusion strategy. FGN with the strategy of fine-tuning and freezing BERT in different stages outperforms the FGN with a trainable BERT. Using Slice-Attention outperforms using average pooling or max pooling in FGN, as Slice-Attention adaptively balances information of each slices but pooling layer only filter information statically. Using sliding window outperforms directly computing outer product of two vectors with a boost of 0.42% in F1. It confirms that sliding window not only reduces the dimension of output vector from outer product, but also enhances the performance of interactive information extraction. Further, Sliding window with the default setting (Section 4.1) slightly outperforms other hyper-parameter settings.

### Vision-based NER

We build a network, using only glyph representation from CGS-CNN with a BiLSTM-CRF without any distributed representations. This method obtains a F1 of 91.12% on Resume dataset, and the LSTM-CRF with initialized character embedding only obtains F1 of 87.15%. The results further conform the effectiveness of glyph information, also shows the feasibility of directly regarding texts as graphs for NER.

## 5 Conclusion

In this paper, we focus on extracting Chinese glyph information and fusing it into character representation. Analyzing and reforming some existing works of both multimodal representation and glyph representation, we propose the FGN for Chinese NER. In FGN, a novel CNN structure called CGS-CNN was applied to encode glyph information from both character graph itself and neighboring graphs of this character. Then a fusion method with out-of-sync sliding window and Slice-Attention is used to fuse two output vectors of BERT and CGS-CNN, which may offer interactive information for NER task. Experiments are conducted on four NER datasets, showing that FGN with LSTM-CRF as tagger obtained SOAT performance on all four datasets. Further, influences of various settings and components in FGN are discussed during ablation study. Specially, we show the feasibility of vision-based NER method.

## Acknowledgments

This work was supported by the National Natural Science Foundation of China (No. 61572145) and the Major Projects of Guangdong Education Department for Foundation Research and Applied Research (No. 2017KZDXM031). The authors would like to thank the anonymous reviewers for their valuable comments and suggestions.

## References

[Devlin et al., 2019]Jacob Devlin, Ming-Wei Chang, Kenton Lee, Kristina Toutanova. BERT: Pre-training of Deep Bidirectional Transformers for Language Understanding. In *Conference of the North American Chapter of the Association for Computational Linguistics (NAACL)*, 4171-4186, 2019.

[Li et al., 2014]Haibo Li, Masato Hagiwara, Qi Li, and Heng Ji. Comparison of the impact of word segmentation on name tagging for Chinese and Japanese. In *International Conference on Language Resources and Evaluation (LREC)*, 2532–2536, 2014.

[Sun et al., 2014] Yaming Sun, Lei Lin, Duyu Tang, Nan Yang, Zhenzhou Ji, Xiaolong Wang. Radical-Enhanced Chinese Character Embedding. In *International Conference on Neural Information Processing (ICONIP)*, 279-286, 2014.

[Dai and Cai, 2017]Falcon Z Dai and Zheng Cai. Glyph-aware embedding of chinese characters. In *Proceedings of the First Workshop on Subword and Character Level Models in NLP*, 64-69, 2017.

[Shao et al., 2017]Yan Shao, Christian Hardmeier, Jorg Tiedemann, and Joakim Nivre. Character-based joint segmentation and pos tagging for chinese using bidirectional rnns-crf. *arXiv:1704.01314*, Computer Science, 2017.

[Ma and Hovy, 2016]Xuezhe Ma, and Eduard Hovy. "End-to-end Sequence Labeling via Bi-directional LSTM-CNNs-CRF. In *Proceedings of the Annual Meeting of the Association for Computational Linguistics (ACL)*, 1064-1074, 2016.

[Meng et al., 2019]Yuxian Meng, Wei Wu, Fei Wang, Xiaoya Li, Ping Nie, Fan Yin, Muyu Li, Qinghong Han, Xiaofei Sun and Jiwei Li. Glyce:Glyph-vectors for Chinese Character Representations. In *Advances in Neural Information Processing Systems (NIPS)*, 2742-2753, 2019.

[Vaswani et al., 2017] Ashish Vaswani, Noam Shazeer, Niki Parmar, Jakob Uszkoreit, Llion Jones, Aidan N. Gomez, Łukasz Kaiser and Illia Polosukhin. Attention is all you need. In *Advances in neural information processing systems*, 5998-6008, 2017.

[Zadeh et al., 2017]Amir Zadeh, Minghai Chen, Soujanya Poria, Erik Cambria, and Louis Philippe Morency. Tensor fusion network for multimodal sentiment analysis. In *Proceedings of the Conference on Empirical Methods on Natural Language Processing (EMNLP)*, 1114–1125, 2017.

[Zadeh et al., 2018]Amir Zadeh, Paul Pu Liang, Navonil Mazumder, Soujanya Poria, Erik Cambria, and Louis Philippe Morency. Memory fusion network for multi-view sequential learning. In *Proceedings of the AAAI Conference on Artificial Intelligence (AAAI)*, 2018

[Mai et al., 2019]Sijie Mai, Haifeng Hu, and Songlong Xing. Divide, Conquer and Combine: Hierarchical Feature Fusion Network with Local and Global Perspectives for Multimodal Affective Computing. In *Annual Meeting of the Association for Computational Linguistics (ACL)*, 481-492, 2019.

[Collobert et al., 2011]Ronan Collobert, Jason Weston, Leon Bottou, Michael Karlen, Koray Kavukcuoglu, and Pavel Kuksa. Natural language processing (almost) from scratch. *Journal of Machine Learning Research*, 12(Aug):2493–2537, 2011.

[Huang Z et al., 2015]Huang Z, Xu W, Yu K. Bidirectional LSTM-CRF models for sequence tagging. *arXiv: 1508.01991*, Computer Science, 2015.

[Lu et al., 2016]Yanan Lu, Yue Zhang, and Dong-Hong Ji. Multi-prototype Chinese character embedding. In *Conference on Language Resources and Evaluation (LREC)*, 2016, 855-859.

[Liu et al., 2010]Zhangxun Liu, Conghui Zhu, and Tiejun Zhao. Chinese named entity recognition with a sequence labeling approach: based on characters, or based on words? *Advanced Intelligent Computing Theories and Applications*, 634–640, 2010.

[Dai et al., 2019]Zeyu Dai, Hongliang Fei and Ping Li. Coreference aware representation learning for neural named entity recognition. In *Proceedings of the International Joint Conference on Artificial Intelligence (IJCAI)*, 4946-4953, 2019.

[Dong et al., 2016]Chuanhai Dong, Jiajun Zhang, Chengqing Zong, Masanori Hattori, and Hui Di. Character-Based LSTM-CRF with Radical-Level Features for Chinese Named Entity Recognition. In *Conference on Natural Language Processing and Chinese Computing (NLPCC)*, 239-250, 2016

[Zhang and Yang, 2018]Yue Zhang and Jie Yang. Chinese NER Using Lattice LSTM. In *Proceedings of the Annual Meeting of the Association for Computational Linguistics (ACL)*, 1554-1564, 2018

[Liu et al., 2019]Wei Liu, Tongge Xu, Qinghua Xu, Jia Song, Yueran Zu. An Encoding Strategy Based Word-Character LSTM for Chinese NER, In *Proceedings of Conference of the North American Chapter of the Association for Computational Linguistics (NAACL)*, 2379-2389, 2019.

[Zhang et al., 2018]Qi Zhang, Jinlan Fu, Xiaoyu Liu, Xuanjing Huang. Adaptive co-attention network for named entity recognition in tweets. In *Proceedings of the AAAI Conference on Artificial Intelligence (AAAI)*, 5674-5681, 2018

[Yu and Jiang, 2019]Jianfei Yu and Jing Jiang. Adapting BERT for Target-Oriented Multimodal Sentiment Classification. In *Proceedings of the International Joint Conference on Artificial Intelligence (IJCAI)*, 5408-5414, 2019.

[Ji et al., 2012]Shuiwang Ji, Wei Xu, Ming Yang, Kai Yu. 3D convolutional neural networks for human action recognition. *IEEE transactions on pattern analysis and machine intelligence*, 35(1): 221-231, 2012.